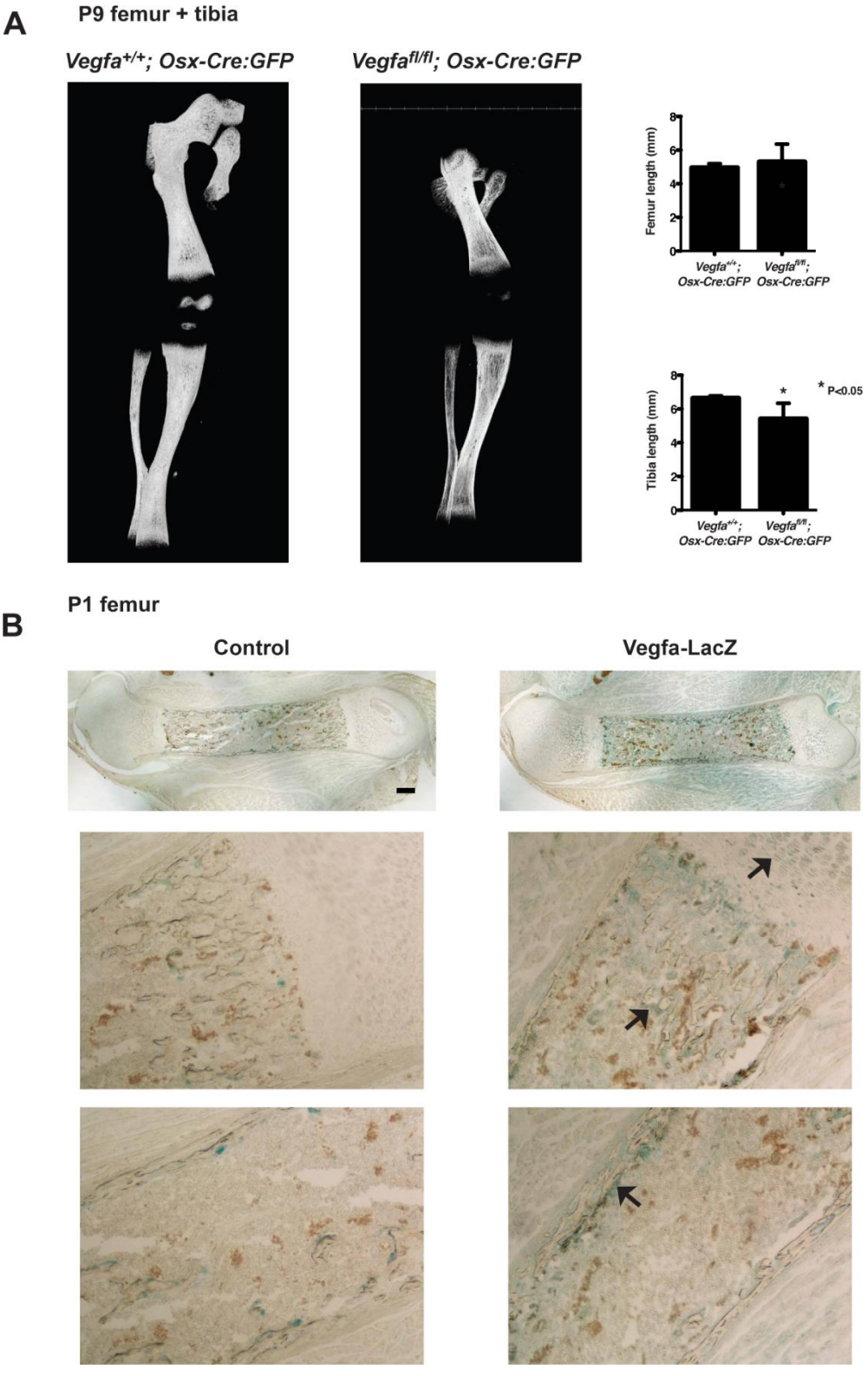
A
P9 femur + tibia
Vegfa+/+; Osx-Cre:GFP
Vegfafl/fl; Osx-Cre:GFP
Femur length (mm)
Vegfa+/+; Osx-Cre:GFP
Vegfafl/fl; Osx-Cre:GFP
Tibia length (mm)
* P<0.05
Vegfa+/+; Osx-Cre:GFP
Vegfafl/fl; Osx-Cre:GFP
B
P1 femur
Control
Vegfa-LacZ

Fig. S1. Progenitor-derived Vegfa regulates the length of early postnatal tibia.

(A) Micro-CT 3D scans of hindlimbs from P9 *Vegfa*$^{+/+}$*; Osx-Cre:GFP* (control, left) and *Vegfa*$^{fl/fl}$*; Osx-Cre:GFP* (mutant, middle) mice. Graphs: Quantification of femur length (mm) (upper right) and tibia length (mm) (lower right) of P9 *Vegfa*$^{+/+}$*; Osx-Cre:GFP* (n=4) and *Vegfa*$^{fl/fl}$*; Osx-Cre:GFP* (n=5) mice. Values represent mean length measures ± s.d.. $P<0.05$ for comparison between genotypes. Note that because of the variable bending between the femur and tibia, the two-dimensional projection as shown here does not constitute the measures of the length of the bones. (B) LacZ staining indicating *Vegfa*-expressing cells in P1 femur of Vegfa-lacZ mice (right) compared with WT control tissue (left) (scale bar: 200 μm). Bottom: Magnified views of POC and prehypertrophic areas of femoral areas showing *Vegfa*-positive cells (arrows).

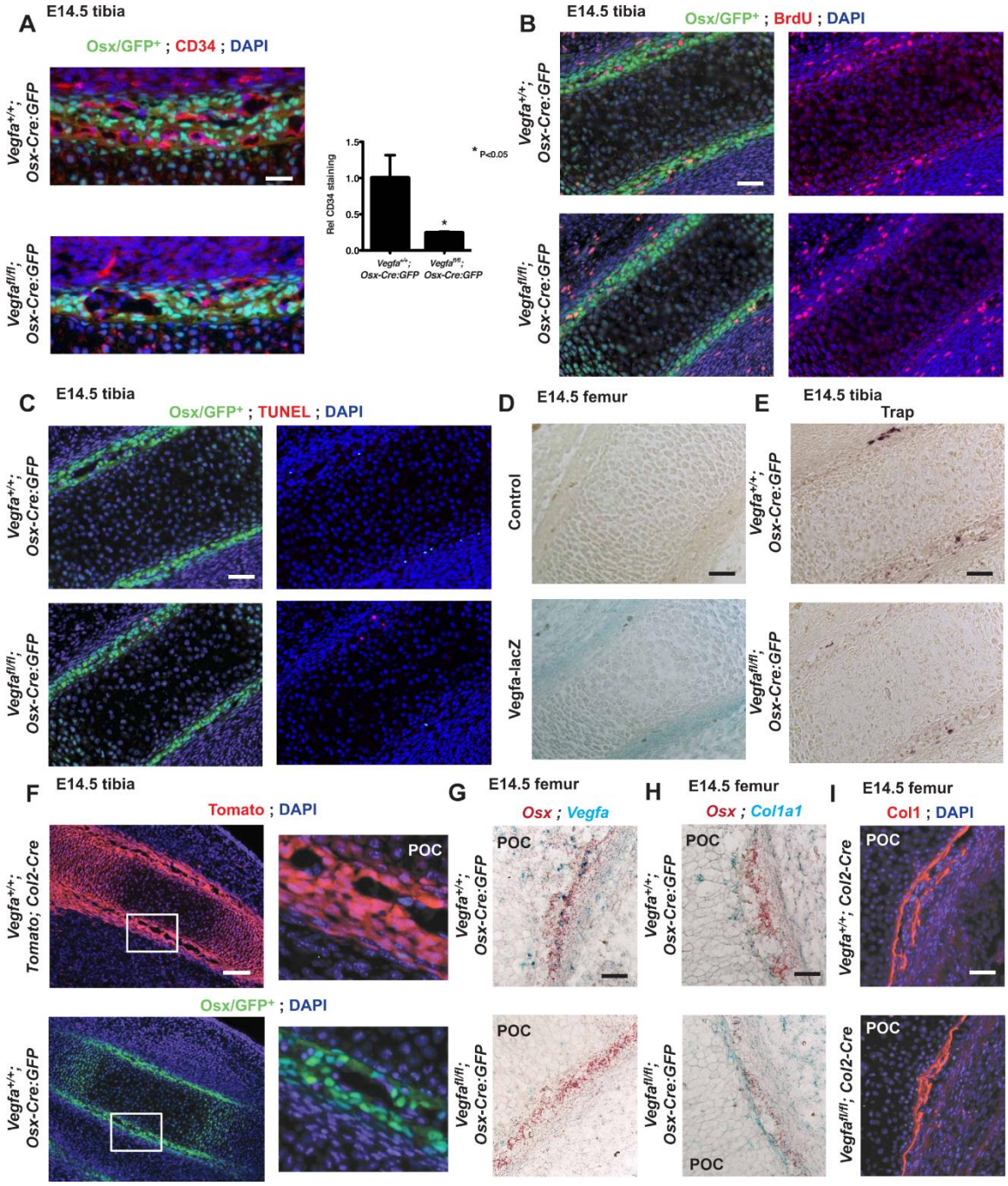
A
E14.5 tibia
Osx/GFP+ ; CD34 ; DAPI
Vegfa+/+; Osx-Cre:GFP
Vegfafl/fl; Osx-Cre:GFP
Rel CD34 staining
1.5
1.0
0.5
0.0
*
*P<0.05
Vegfa+/+; Osx-Cre:GFP
Vegfafl/fl; Osx-Cre:GFP
B
E14.5 tibia
Osx/GFP+ ; BrdU ; DAPI
Vegfa+/+; Osx-Cre:GFP
Vegfafl/fl; Osx-Cre:GFP
C
E14.5 tibia
Osx/GFP+ ; TUNEL ; DAPI
Vegfa+/+; Osx-Cre:GFP
Vegfafl/fl; Osx-Cre:GFP
D
E14.5 femur
Control
Vegfa-lacZ
E
E14.5 tibia
Trap
Vegfa+/+; Osx-Cre:GFP
Vegfafl/fl; Osx-Cre:GFP
F
E14.5 tibia
Tomato ; DAPI
Vegfa+/+; Tomato; Col2-Cre
POC
Osx/GFP+ ; DAPI
Vegfa+/+; Osx-Cre:GFP
G
E14.5 femur
Osx ; Vegfa
POC
Vegfa+/+; Osx-Cre:GFP
Vegfafl/fl; Osx-Cre:GFP
H
E14.5 femur
Osx ; Col1a1
POC
Vegfa+/+; Osx-Cre:GFP
Vegfafl/fl; Osx-Cre:GFP
I
E14.5 femur
Col1 ; DAPI
POC
Vegfa+/+; Col2-Cre
Vegfafl/fl; Col2-Cre

Fig. S2. Loss of progenitor-derived Vegfa does not affect the proliferation and apoptosis of Osx$^+$ cells in perichondrial areas.

(A) Anti-CD34 staining of perichondrial areas of tibia sections of *Vegfa*$^{+/+}$*; Osx-Cre:GFP* and *Vegfa*$^{fl/fl}$*; Osx-Cre:GFP* mice (scale bar: 25 μm). Right: Quantification of anti-CD34 staining in perichondrium of E14.5 tibia of *Vegfa*$^{+/+}$*; Osx-Cre:GFP* (n=3) and *Vegfa*$^{fl/fl}$*; Osx-Cre:GFP* (n=3) mice. Values represent mean relative anti-CD34 staining ± s.d.. P<0.05 for comparison between genotypes. (B) BrdU staining of tibia sections from E14.5 *Vegfa*$^{+/+}$*; Osx-Cre:GFP* (top) and *Vegfa*$^{fl/fl}$*; Osx-Cre:GFP* (bottom) mice showing Osx/GFP+ cells in perichondrial areas of tibia (scale bar: 50 μm). Right: Identical images showing BrdU staining only. (C) TUNEL staining of tibia sections from E14.5 *Vegfa*$^{+/+}$*; Osx-Cre:GFP* (top) and *Vegfa*$^{fl/fl}$*; Osx-Cre:GFP* (bottom) mice showing Osx/GFP$^+$ cells in perichondrial areas of tibia (scale bar: 50 μm). Right: Identical images showing TUNEL staining only. (D) LacZ staining indicating *Vegfa*-expressing cells in E14.5 femur of Vegfa-LacZ mice (bottom) compared to no background staining in tissue from WT control mice (top) (scale bar: 50 μm). (E) Trap staining of tibia sections from E14.5 *Vegfa*$^{+/+}$*; Osx-Cre:GFP* (top) and *Vegfa*$^{fl/fl}$*; Osx-Cre:GFP* (bottom) mice showing osteoclasts in perichondrial areas of tibia (scale bar: 50 μm). (F) Analysis of different cell populations located in perichondrium of E14.5 tibia. Top: Tibia section from E14.5 *Vegfa*$^{+/+}$*; Tomato; Col2-Cre* mice showing cells derived from osteochondroprogenitor (Col2$^+$) cells (scale bar: 100 μm). Bottom: Tibia from *Vegfa*$^{+/+}$*; Osx-Cre:GFP* mice showing Osx-expressing cells. Right: Magnified views of delineated rectangular areas of perichondrium in images on left. (G) *In situ* hybridization on femur sections of E14.5 *Vegfa*$^{+/+}$*; Osx-Cre:GFP* (top) and *Vegfa*$^{fl/fl}$*; Osx-Cre:GFP* (bottom) mice for *Osx* (red spots) and *Vegfa* (turquoise spots) (scale bar: 50 μm). (H) *In situ* hybridization on femur sections of E14.5 *Vegfa*$^{+/+}$*; Osx-Cre:GFP* (top) and *Vegfa*$^{fl/fl}$*; Osx-Cre:GFP* (bottom) mice for *Osx* (red spots) and *Col1a1* (turquoise spots) (scale bar: 50 μm). (I) Anti-Col1 staining of

femur sections from E14.5 *Vegfa*$^{fl/fl}$*; Col2-Cre* (bottom) and WT control (top) mice showing Col1 deposition in perichondrial area at center of femur (scale bar: 50 μm).

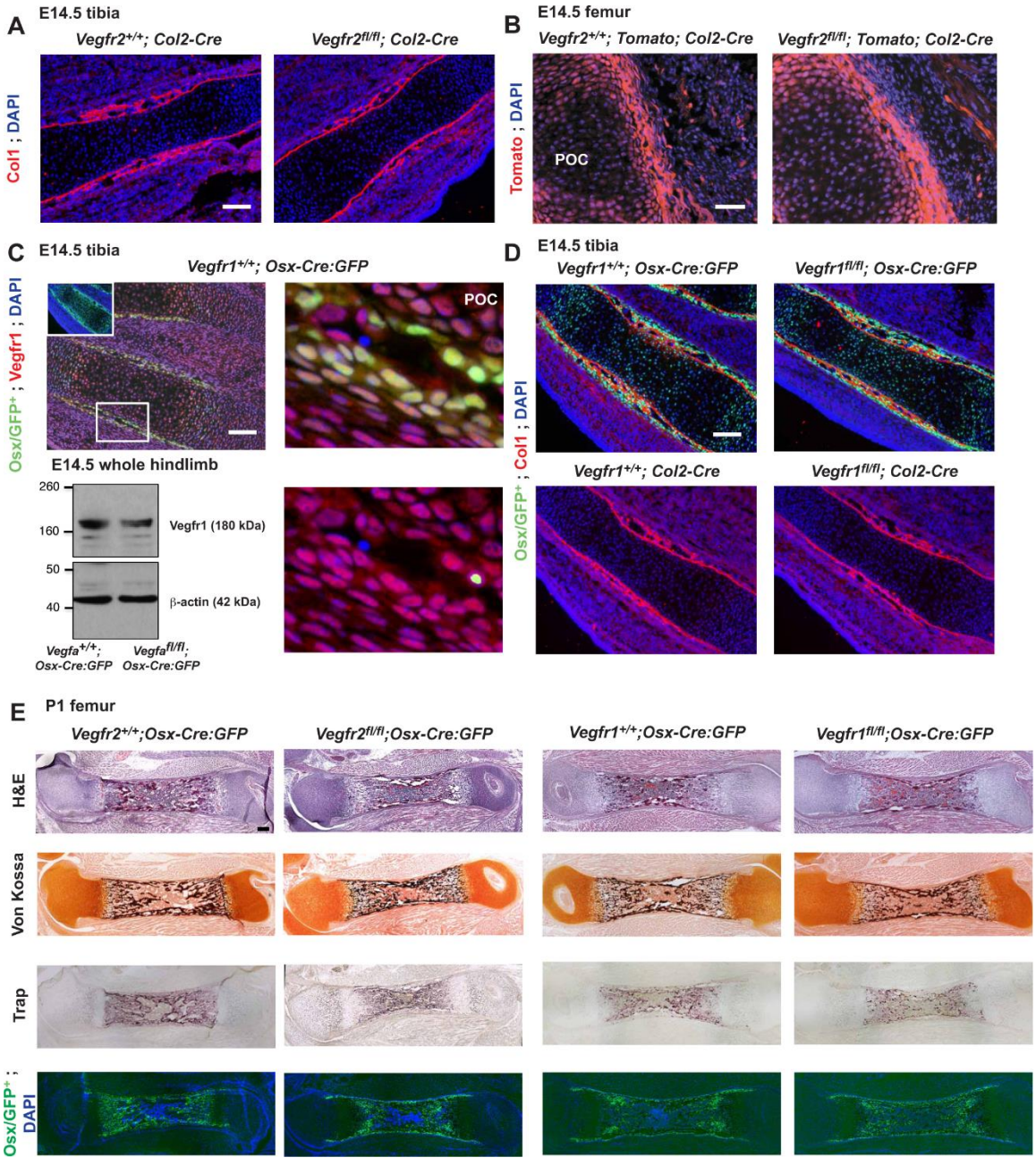
A
E14.5 tibia
Vegfr2+/+; Col2-Cre
Vegfr2fl/fl; Col2-Cre
Col1 ; DAPI
B
E14.5 femur
Vegfr2+/+; Tomato; Col2-Cre
Vegfr2fl/fl; Tomato; Col2-Cre
Tomato ; DAPI
POC
C
E14.5 tibia
Vegfr1+/+; Osx-Cre:GFP
Osx/GFP+ ; Vegfr1 ; DAPI
POC
E14.5 whole hindlimb
260
160
Vegfr1 (180 kDa)
50
40
β-actin (42 kDa)
Vegfa+/+; Osx-Cre:GFP
Vegfafl/fl; Osx-Cre:GFP
D
E14.5 tibia
Vegfr1+/+; Osx-Cre:GFP
Vegfr1fl/fl; Osx-Cre:GFP
Osx/GFP+ ; Col1 ; DAPI
Vegfr1+/+; Col2-Cre
Vegfr1fl/fl; Col2-Cre
E
P1 femur
Vegfr2+/+;Osx-Cre:GFP
Vegfr2fl/fl;Osx-Cre:GFP
Vegfr1+/+;Osx-Cre:GFP
Vegfr1fl/fl;Osx-Cre:GFP
H&E
Von Kossa
Trap
Osx/GFP+ ; DAPI

Fig. S3. Loss of Vegfr1 in osteoprogenitor cells does not affect osteoblast differentiation in perichondrium and mineralization of developing bones.

(A) Anti-Col1 staining of tibia sections from E14.5 *Vegfr2*$^{+/+}$*; Col2-Cre* (left) and *Vegfr2*$^{fl/fl}$*; Col2-Cre* (right) mice (scale bar: 100 μm). (B) Femur sections from E14.5 *Vegfr2*$^{+/+}$*; Tomato; Col2-Cre* (left) and *Vegfr2*$^{fl/fl}$*; Tomato; Col2-Cre* (right) mice showing cells derived from osteochondroprogenitor (Col2^{+}) cells (scale bar: 50 μm). (C) Top left: Anti-Vegfr1 staining of tibia sections from E14.5 *Vegfr1*$^{+/+}$*; Osx-Cre:GFP* mice showing Osx/GFP^{+} cells in the perichondrium with insert showing non-immune IgG control (scale bar: 100 μm). Top right: Magnified view of delineated rectangular area at left showing Osx/GFP^{+} cells (green) and identical images with Vegfr1 staining only (bottom right). Bottom left: Western blotting of Vegfr1 protein levels in whole hindlimb lysates from E14.5 *Vegfa*$^{+/+}$*; Osx-Cre:GFP* (control) and *Vegfa*$^{fl/fl}$*; Osx-Cre:GFP* (mutant) mice; β-actin is loading control. (D) Anti-Col1 staining of femur sections from E14.5 *Vegfr1*$^{+/+}$*; Osx-Cre:GFP* (top left) and *Vegfr1*$^{fl/fl}$*; Osx-Cre:GFP* (top right) and femur sections from *Vegfr1*$^{+/+}$*; Col2-Cre* (bottom left) and *Vegfr1*$^{fl/fl}$*; Col2-Cre* (bottom right) mice (scale bar: 100 μm). (E) Histological analysis of femur sections from P1 *Vegfr2*$^{fl/fl}$*; Osx-Cre:GFP* (left) and *Vegfr1*$^{fl/fl}$*; Osx-Cre:GFP* (right) compared to WT littermate control mice by H&E, Von Kossa, Trap and Osx/GFP^{+} expression (scale bar: 200 μm).

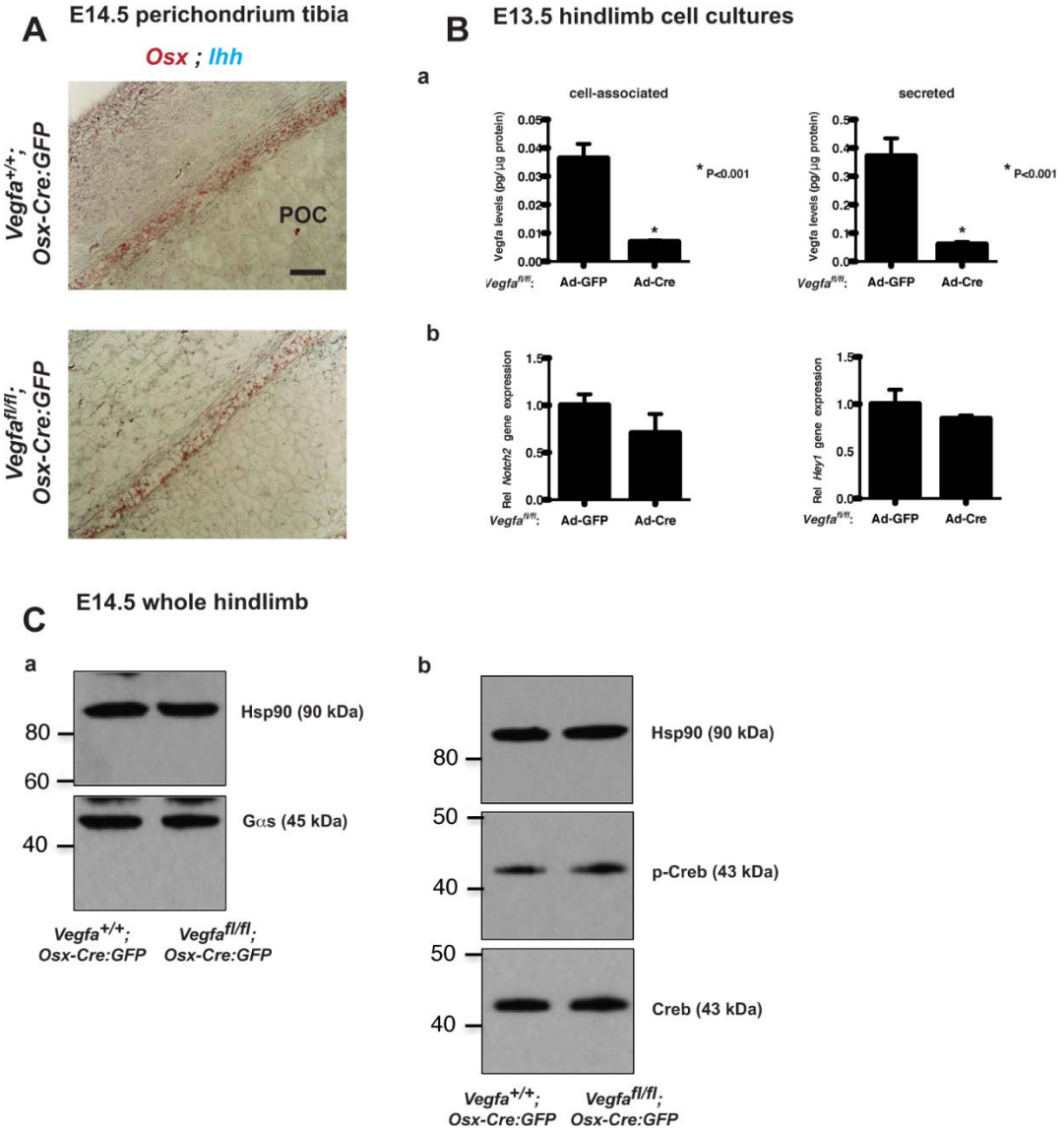
A
E14.5 perichondrium tibia
Osx ; Ihh
Vegfa+/+; Osx-Cre:GFP
POC
Vegfafl/fl; Osx-Cre:GFP
B
E13.5 hindlimb cell cultures
a
cell-associated
secreted
Vegfa levels (pg/µg protein)
* P<0.001
Vegfafl/fl:
Ad-GFP
Ad-Cre
b
Rel Notch2 gene expression
Rel Hey1 gene expression
C
E14.5 whole hindlimb
a
Hsp90 (90 kDa)
Gαs (45 kDa)
Vegfa+/+; Osx-Cre:GFP
Vegfafl/fl; Osx-Cre:GFP
b
Hsp90 (90 kDa)
p-Creb (43 kDa)
Creb (43 kDa)

Fig. S4. Vegfa does not affect perichondrial Ihh expression and Gαs and Pka-dependent pathways

(A) *In situ* hybridization on tibia sections (perichondrium area) from E14.5 *Vegfa*$^{+/+}$*; Osx-Cre:GFP* (top) and *Vegfa*$^{fl/fl}$*; Osx-Cre:GFP* (bottom) mice for *Osx* (red spots) and *Ihh* (turquoise spots) (scale bar: 50 μm). (B) (a) Vegfa protein levels measured by ELISA in cell-associated and secreted protein lysates of cultured hindlimb cells isolated from E13.5 *Vegfa*$^{fl/fl}$ embryos treated with adenoviral Cre compared to adenoviral GFP (control). Vegfa protein levels normalized to total cellular proteins for each sample. Values represent mean Vegfa levels ± s.d. (n=3). (b) qRT-PCR of *Notch2* and *Hey1* expression in cultured hindlimb cells isolated from E13.5 *Vegfa*$^{fl/fl}$ embryos, treated with adenoviral Cre, and induced to differentiate into the osteoblast lineage. Control cells were treated with adenoviral GFP. Relative gene expression levels normalized to levels of *Gapdh*. Values represent mean relative expression ± s.d. (n=3). (C) Western blotting of Gαs (a) and phospho-Creb (Ser133) (b) in whole hindlimb lysates from E14.5 *Vegfa*$^{+/+}$*; Osx-Cre:GFP* (control) and *Vegfa*$^{fl/fl}$*; Osx-Cre:GFP* (mutant) mice; Hsp90 is loading control.

Supplementary Materials and Methods

Mouse Strains

Floxed *Vegfa*, *Flk1* and *Flt1* mice were crossed with Osx-Cre:GFP and described in our previous studies (Liu et al., 2012). Here we used additional crosses of mice carrying floxed alleles of *Vegfa*, *Flk1* and *Flt1* with *Col2-Cre*. Adult heterozygous 129-*Vegfatm1.1Nagy* mice were previously reported to have increased Vegfa protein levels as a consequence of the insertion of an IRES-NLS-lacZ-SV40pA sequence into the 3' UTR of the *Vegfa* gene locus resulting in removal of miRNA binding sites controlling inhibition of *Vegfa* mRNA translation (Cervi et al., 2007; Miquerol et al., 1999; Marneros, 2013). Analysis of whole hindlimb lysates from E14.5 129-*Vegfatm1.1Nagy* mice by Western blotting and ELISA assays showed that Vegfa protein levels were not significantly different from E14.5 WT controls (data not shown). For all timed pregnancies, male mice were mated with females overnight and separated in the morning, which was defined as E0.5. For harvesting of embryos, timed pregnant female mice were sacrificed by CO_2 exposure and the embryos were harvested after amnionectomy and removal of placenta. Genomic DNA isolated from portions of mouse tails were used for genotyping. All primers for genotyping are listed below.

Primer sequences used for genotyping

	forward primer	**reverse primer**	Product
Generic-Cre	5′-GATGAGGTTCGCAAGAACCTG-3′	5′-TGAACGAACCTGGTCGAAATC-3′	~ 350 bp
Vegfa	5′-CCTGGCCCTCAAGTACACCTT-3′	5′-TCCGTACGACGCATTTCTAG-3′	~ 150 bp
Vegfr1	5′-CCTGCATGATTCCTGATTGGA-3′	5′-GCCTAAGCTCACCTGCGG-3′	~ 180 bp
Vegfr2	5′-GACTTGGTTCATCAGGCTAG-3′	5′-GACGCTGTTAAGCTGCTACAC-3′	~ 230 bp
Vegfa-LacZ	5′-ATCCTCTGCATGGTCAGGTC-3′	5′-CGTGGCCTGATTCATTCC-3′	~ 300 bp
Vegfa-LacZ (positive control)	5′-CAAATGTTGCTTGTCTGGTG-3′	5′-GTCAGTCGAGTGACAGTTT-3′	~ 260 bp

Rosa Wildtype	5′-AAGGGAGCTGCAGTGGAGTA-3′	5′-CCGAAAATCTGTGGGAAGTC-3′	~ 297 bp
Rosa Tomato Mutant	5′-CTGTTCCTGTACGGCATGG-3′	5′-GGCATTAAAGCAGCGTATCC-3′	~ 169 bp

Skeletal Preparations and Staining

Skeletal structures of newborn mice (P1) were visualized by Alizarin Red (bone) and Alcian Blue (cartilage) staining. Skin, muscles and visceral organs were removed from mice prior to incubation in solution containing Alizarin Red S and Alcian Blue (Sigma-Aldrich). Skeletal samples were cleared by incubation in potassium hydroxide (1%) /glycerol (20%) solution and stored and photographed in glycerol.

Histology

Limbs of embryos and newborn mice were fixed in 4% paraformaldehyde (PFA) at 4°C overnight, infiltrated with 10%, 20% and 30% sucrose and embedded in OCT (Tissue-Tek®) compound (Sakura Finetek USA, Inc., Torrance, CA) for cryostat sectioning. 7.5 μm frozen sections were prepared for hematoxylin and eosin (H&E) staining, von Kossa staining, tartrate-resistant acid phosphatase (Trap) staining, bromodeoxyuridine (BrdU) staining, TUNEL staining and immunohistochemistry (IHC). For detection of mineralization, Von Kossa staining was performed by placing the frozen sections in 1% silver nitrate under a 60 Watt lamp for 90 minutes. The reaction was then stopped by putting sections in 2.5% sodium thiosulfate solution for 5 minutes and counterstained with 1% Safranin O solution. Trap staining for osteoclasts was performed using a Leukocyte Acid Phosphatase kit (Sigma-Aldrich) according to the manufacturer's instructions. Histological sections were taken with Nikon 80i Upright microscope using NIS-Elements AR3.1 software.

Immunohistochemistry (IHC) and immunocytochemistry (ICH)

IHC was performed according to Cell Signaling Technology protocols. Frozen sections of limbs were stained with CD31 (1:100; ab28364; Abcam), CD34 (1:100; ab81289; Abcam), Collagen I (1:100; ab21286; Abcam), Vegfr2 (1:50; sc-505; Santa Cruz Biotechnology), Vegfr1 (1:50; sc-316; Santa Cruz Biotechnology), β-catenin (1:500; C2206; Sigma-Aldrich) and Notch2 (1:1500; 5732; Cell Signaling) primary antibodies or normal rabbit IgG (sc-2027; Santa Cruz Biotechnology), and Alexa Fluor-conjugated secondary antibodies (1:200; Invitrogen). For ICH cells in culture chambers were fixed in 4% PFA and stained with Vegfa (1:50; sc-152; Santa Cruz Biotechnology) and Osx (1:50; sc-22538; Santa Cruz Biotechnology) primary antibodies, and Alexa Fluor-conjugated secondary antibodies (1:200; Invitrogen). All sections were mounted with HardSet Mounting Medium with DAPI (Vector Labs), observed and photographed using Nikon 80i Upright microscope or a Nikon Ti w/ Spinning Disk Confocal microscope. Control sections incubated with non-specific control IgGs did not show any staining. Images of the same optic fields were taken using blue, green and/or red fluorescence filters, and merged using MetaMorph Software.

X-Gal Staining

To detect Vegfa-lacZ reporter expression indicating *Vegfa* expression, E14.5 embryos or hindlimbs of newborn mice were fixed in 0.2% glutaraldehyde (EMS) and 2% PFA (BDH) for 30 minutes at room temperature, incubated in X-gal solution (1 mg/ml; Thermo Scientific) overnight at 30°C and post-fixed in 10% PFA overnight at room temperature. The bones were washed for 30 minutes in running water and then processed using a standard procedure for frozen sections.

RNA in situ hybridization

Frozen sections of limbs were processed for RNA in situ detection using the RNAscope 2-plex Detection Kit (Chromogenic) according to the manufacturer's instructions (Advanced Cell Diagnostics). RNAscope probes used include: Sp7 (NM_130458.3, region 837-2230), which was detected using the Fast Red detection reagent, and Col1a1 (NM_007742.3, region 1685-3051), Indian hedgehog (NM_010544.2, region 990-2336), Vegfa (NM_001025257.3, region 946-2156) and Col2a1 (NM_001113515.2, region 729-2036), which were detected using the Green detection reagent.

MicroCT

μCT analyses were performed for hindlimbs of P9 mice using μCT40 Scanco Medical, Zurich, Switzerland (10 mm isometric voxel resolution at 200 mseconds exposure, 2000 views and 5 frames per view).

Quantification of femur diameter, mineralization, Osx-Positive Cells, Trap staining, CD31 staining, CD34 staining, and Col1 staining

Diameter of P1 femurs was measured on four central-cut sections at least 30 μm apart (n=3 animals per genotype). The total areas of mineralization, Trap staining and Osx/GFP-positive cells in P1 femurs were measured on the entire diaphysis of the femur, using ImageJ program. Three central-cut sections at least 22.5 μm apart were analyzed per bone (n=3 animals per genotype). The invasion of endothelial cells and osteoclasts into the primary ossification center of E15.5 femurs were analyzed by comparing anti-CD31 staining and Trap staining in the primary ossification center of femur and total staining in a defined (Trap: 1100 x 1100 μm; CD31: 1150 x 1150 μm) region comprising the diaphysis of the femur. Three central-cut sections at least 22.5 μm apart were analyzed per bone (n=3 embryos per genotype). Osx-positive cells in E14.5 and E15.5 tibia sections were counted in a defined (80 x 330 μm) region comprising most of the

perichondrium, using ImageJ program. Three to six central-cut sections at least 22.5 μm apart were analyzed per bone (n=3 embryos per genotype). CD31 and CD34 stainings of E14.5 tibia sections were analyzed in a defined (190 x 1850 μm) region comprising most of the perichondrium, using ImageJ program. Three sections at least 22.5 μm apart were analyzed per bone (n=3 embryos per genotype). Col1 staining of E14.5 femur sections was analyzed in a defined (370 x 1480 μm) region comprising most of the perichondrium, using ImageJ program. Four to seven sections at least 30 μm apart were analyzed per bone (n=3 embryos per genotype).

Western Blotting

Protein lysates of hindlimbs of E14.5 embryos were prepared by adding ice-cold M-PER Mammalian Protein Extraction Reagent (Thermo Scientific) supplemented with cOmplete, Mini, EDTA-free protease inhibitor (Roche) and PhosSTOP phosphatase inhibitors (Roche). After centrifugation for 10 minutes (14,000 *rpm)* at 4°C, protein concentrations of supernatants were determined by Bradford Protein Assay kit (Thermo Scientific). Equal amounts of lysates were loaded and separated by SDS-polyacrylamide gel electrophoresis using 4-12% Bis-Tris precast polyacrylamide gels (NuPage; Invitrogen) followed by transfer of proteins onto nitrocellulose membranes (Bio-Rad). Protein was detected by probing the membranes overnight at 4°C using primary antibodies against phospho-Vegfr2 (1:1000; 2478; Cell Signaling), Vegfr2 (1:1000; 2479; Cell Signaling), Vegfr1 (1:500; sc-316; Santa Cruz Biotechnology), Ihh (1:1000; ab39634; Abcam), Gαs (1:500; sc-135914; Santa Cruz Biotechnology), phospho-Akt (1:1000; 9271; Cell Signaling), Akt (1:1000; 9272; Cell Signaling), phospho-Creb (1:1000; 9198; Cell Signaling), Creb (1:1000; 9197; Cell Signaling), β-catenin (1:1000; 9587; Cell Signaling), phospho-Gsk3β (1:1000; 9323; Cell Signaling), Gsk3β (1:1000; 9315; Cell Signaling), Notch2 (1:1000; 5732; Cell Signaling), phospho-p44/42 Mapk (1:1000; 9101; Cell Signaling), p44/42 Mapk (1:1000; 9102; Cell Signaling), Hsp90 (1:500; sc-13119; Santa Cruz Biotechnology), and β-actin

(1:5000; A5441; Sigma-Aldrich). Membranes were then incubated with horseradish peroxidase-conjugated secondary antibodies for 1 hour at room temperature and immunoreactive bands were detected by chemiluminescent substrate (Thermo Scientific).

BrdU incorporation and TUNEL staining

For BrdU incorporation, pregnant mice were injected i.p. with BrdU (Invitrogen) at 0.1 mg/g body weight two hours before sacrifice. E14.5 embryos were dissected and their limbs processed to obtain frozen sections. BrdU staining was performed using BrdU Staining Kit (Invitrogen) following manufacturer's instructions. For TUNEL staining, apoptotic cells were detected by using In Situ Cell Death Detection Kit, TMR Red (Roche) as described in manufacturer's instructions.

Mesenchymal Progenitor Cell Cultures

Hindlimbs of E13.5 embryos were dissected in Hanks Balanced Salt Solution (HBSS, Sigma-Aldrich) and digested in collagenase II (0.37 mg/ml), 0.25% dextrose in HBSS at 37°C for 90 minutes. Cells were disassociated by repetitive pipetting, centrifuged, resuspended in BGJb medium (Life Technologies) supplemented with 10% FBS, 1 x Antibiotics (Gibco), and plated in 12-well plates at 5 x 10^5 cells per well. Prior to reaching confluence cells were infected with either Ad-Cre or Ad-GFP overnight (Vector Biolabs). Cells were grown to confluence, induced to differentiate in the presence of β-glycerophosphate (8 mM; Sigma-Aldrich) and L-ascorbic acid phosphate (50 μg/ml; Wako), and cultured for 5 days for Vegfa ELISA assays and 14 days for qRT-PCR. For rescue experiments cells were treated with recombinant mouse Vegfa (Vegf164) (50 ng/ml; 493-MV, R&D Systems) with or without Hedgehog antagonist GANT-58 (5 μM; Sigma-Aldrich).

ELISA assays

Vegfa protein levels in cell lysates were assessed using the Quantikine Mouse VEGF Immunoassay (R&D Systems) in accordance with manufacturer's instructions; Vegfa protein levels assessed in cell lysates (cell-associated) or culture media (secreted) were normalized to total cellular proteins for each sample.

RNA extraction and gene expression analysis by qRT-PCR

Total RNA was extracted from cells using the RNeasy Isolation kit (Qiagen) according to the manufacturer's instructions. Then 1 μg of total RNA was used for cDNA synthesis using the RT^2 Easy First Strand kit (Qiagen) and PCR amplification of cDNA was performed using the iCycler iQ PCR system (Bio-Rad) using gene-specific primer sets listed below. Primers were designed using Primer3 software with parameters set for use with RT-PCR and PCR products were analyzed by gel electrophoresis to ensure the generation of a single product in the PCR reaction. Relative gene expression levels were normalized to the levels of the housekeeping gene *Gapdh*. All primers for qRT-PCR are listed below.

Primer sequences used for qRT-PCR

	forward primer	**reverse primer**
Gapdh	5'-GTGTTCCTACCCCCAATGTG-3'	5'-AGGAGACAACCTGGTCCTCA-3'
Runx2	5'-CCCAGCCACCTTTACCTACA-3'	5'-TATGGAGTGCTGCTGGTCTG-3'
Sp7	5'-AGGCACAAAGAAGCCATACG-3'	5'-TGCAGGAGAGAGGAGTCCAT-3'
Col1a1	5'-TGACTGGAAGAGCGGAGAGT-3'	5'-GTTCGGGCTGATGTACCAGT-3'
Ihh	5'-CCGAACCTTCATCTTGGTGT-3'	5'-CCCCGAGAAACATTGGAGTA-3'
Ptch1	5'-GAGACAAGCCCATCGACATT-3'	5'-CCAAGCGGTCAGGTAGATGT-3'
Gli1	5'-ACTAGGGGGCTACAGGAGGA-3'	5'-ACCTGGACCCCTAGCTTCAT-3'

Hhip	5'-TACTTGCCGAGGCCATATTC-3'	5'-CTTCCATCTGGCCCAAGTAG-3'
Notch2	5'-GATCGACAACCGACAGTGTG-3'	5'-GCGTTTCTTGGACTCTCCAG-3'
Hey1	5'-TGATGGACCGAGGTGTTGTA-3'	5'-TCCCTTCACCTCACTGCTCT-3'

Supplementary References

Cervi, D., Shaked, Y., Haeri, M., Usenko, T., Lee, C.R., Haigh, J.J., Nagy, A., Kerbel, R.S., Yefenof, E., and Ben-David, Y. (2007). Enhanced natural-killer cell and erythropoietic activities in VEGF-A-overexpressing mice delay F-MuLV-induced erythroleukemia. *Blood* **109**, 2139-2146.

Marneros, A.G. (2013). NLRP3 inflammasome blockade inhibits VEGF-A-induced age-related macular degeneration. *Cell Rep*. **4**, 945-958.